

SYSTEM MODELING BASED ANTI-SHAKE MECHANISM FOR MOBILE DISPLAY

JYH-DA WEI^{1,2}, HSU-FU HSIAO¹ AND PEI-YU JIANG¹

¹Department of Computer Science and Information Engineering
College of Engineering

²School of Electrical and Computer Engineering
Chang Gung University

No. 259, Wenhua 1st Rd., Guishan Dist., Taoyuan City 33302, Taiwan
jdwei@mail.cgu.edu.tw; shiftsmart@gmail.com; stage7923@hotmail.com

Received June 2016; revised October 2016

ABSTRACT. *Mobile computing devices facilitate our daily lives; however, mobile display also has adverse impacts on our vision and may even injure our eyes. Mobile devices cause visual discomfort mainly due to handheld shake and vibration, especially when they are used in moving environments. In this paper, we propose an anti-shake mechanism for mobile display. This mechanism is aimed to provide users with a comfortable interaction experience and minimize negative side effects of screen vibrations. The overall process of the anti-shake mechanism includes analyzing the accelerometer data, predicting the magnitude of device displacement, and adjusting the position of the display area to compensate for vibrations. A system modeling based technique was developed as the kernel for motion prediction and display stabilization. We then verified this technique with prediction accuracy test and user evaluation test. The experimental results reveal that our anti-shake mechanism can precisely simulate ground-truth displacement and successfully decrease sight fatigue when applied to mobile devices used in dynamically changing environments.*

Keywords: Mobile device, Mobile display, Stabilization, System modeling, Least square estimation

1. **Introduction.** With the development and progress of science and technology, mobile computing devices, such as smart phones or tablet computers, have become indispensable parts of our lives. According to reports from the International Data Center (IDC, <http://www.idc.com>), worldwide shipments of smart phones and tablet computers reached 1.3 billion and 240 million units, respectively, in 2015. The market for mobile computing devices continuously increased in recent years. This situation also concludes that using mobile computing devices is highly engaged with our everyday lives. Although mobile devices offer great convenience in all aspects of our daily lives [1], many researchers have noticed that these devices could cause negative effects to addicted users (also known as phubbing). Examples of these adverse effects include criminal acts [2, 3] (e.g., violation of privacy, online fraud, random robbery), psychological problems [4, 5] (e.g., rest or sleep disorders, social phobias, Internet addiction) and physiological diseases [6] (e.g., muscular pains, glaucoma, and myopia).

Among these problems, the most frequently encountered include motion sickness [7] and visual damage [8]. When the handheld mobile device is used while the user is walking or in a moving vehicle, the display screen of the mobile device may shake with movement of the user's hand. It is uncomfortable for the user's eyes to view image information displayed on the unsteady display screen. Especially, after continuous viewing of the unsteady display

TABLE 1. Taiwan students who have suffered from vision decline (%)

Year	Primary School	Junior High School	Senior High School
2007	44.89	69.11	84.9
2008	46.70	70.76	85.7
2009	47.86	71.58	86.1
2010	49.1	73.52	86.4
2011	50.01	74.25	86.5
2012	49.36	73.71	86.3
2013	48.11	73.51	86.6
2014	47.06	73.32	86.8

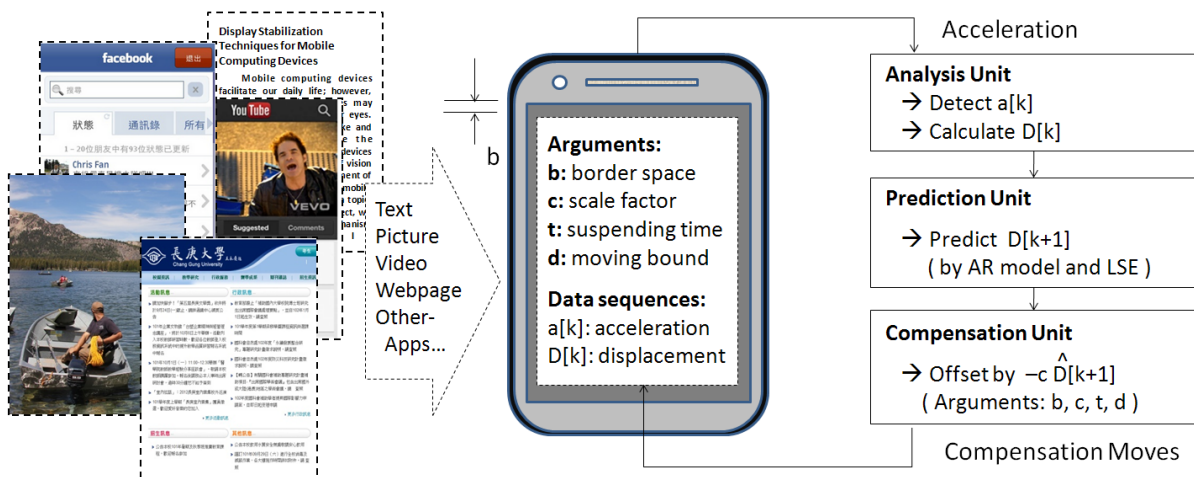


FIGURE 1. Infrastructure of the anti-shake mechanism

screen, the user's eyes may easily feel tired or fatigued, resulting in damages to the eyes, eye diseases or motion sickness. Table 1 lists the percentages of Taiwan students who have suffered from vision decline, i.e., with at least one eye with less than 20/20 vision, verified by examinations. According to the data released by the Ministry of Education in Taiwan (<http://www.edu.tw>), a very high percentage of school children and teenagers have to correct their vision. Serious sight-related problems like this can be attributed to the overuse of mobile computing devices [9].

To relieve eye discomfort and to decrease the risk of visual damage, we assess to implement an anti-shake mechanism for stabilizing mobile displays. Figure 1 illustrates this solution. We set an active area on the screen for displaying the media content, e.g., pictures, text segments, web pages, and the output of other applications. Outside of the active area is a border ring for this display area to move to compensate for device vibrations. In this paper, we propose a system modeling based technique that serves as the kernel to predict the amount of displacement that needs to be compensated for. To validate the proposed method, we first used a high frame rate camera to capture the process while the mobile computer was moved. Analyzing the ground-truth displacement frame by frame, we found our method can trace the move of the device precisely. We then applied this stabilization technique to user evaluation scenarios, which consisted of viewing image, text, and video contents and then going through some exams and questionnaires. The positive feedback from users successively verified the feasibility of this anti-shake mechanism.

The rest of this paper is organized as follows. After we introduced the basic idea in Section 1, we present a survey on the existing stabilization techniques in Section 2. Then, we present the details of our proposed techniques in Section 3. In Section 4, we state the experimental results of prediction accuracy tests. Next in Section 5, we describe the user verification process and discuss the results. Finally, the concluding remarks are presented in Section 6.

2. Related Work. The results obtained from research on the stabilization of media access provide valuable insight. Practical techniques have been developed for image and video capture. In recent years, we can also find some related research that focuses on improving the quality of mobile displays.

2.1. Stabilization techniques for image and video capture. Handheld vibration is a serious problem for digital cameras. Stabilization techniques for image-recording and video-recording were, thus, developed by several notable companies [10, 11]. Canon's image-stabilization (IS) technique and Nikon's vibration-reduction (VR) technique are examples that use damping systems on the camera lens to enhance the image quality when images are captured. A similar method was also developed by Sony and Monica, where the damping mechanism was built on the CCD unit. Apart from hardware solutions, offline processing algorithms were also proposed to decrease video vibrations [12, 13]. These algorithms provide a software solution that aligns and clips subareas in conjoint frames, thereby regenerating a stable video.

Although these techniques perform well for image and video captures, they are not available for mobile device display because a damping screen cannot be attached to the devices and offline post-processing is not possible during its operation. To address the handheld shake problem, we first predict the amount of displacement as a result of the respective motion and then compensate it in the opposite direction.

2.2. Stabilization techniques for mobile displays. Early in 2007, Barnard et al. had noticed that handheld vibrations could interfere with the reading of text in environments in motion [14]. Research that has since been conducted to facilitate the reading of texts on mobile devices includes enlarging the text size dynamically [15] and magnifying the local area that contains the content [16]. The analysis of walk types [17] is also an interesting research field that not only improves the performance of these solutions but also the accuracy of screen touch.

The anti-shake mechanism we implement in this paper is built upon motion compensation. Besides text segments, an implementation like this can display any other kind of media content, although the display area of the screen should be decreased. The original idea behind this implementation can be seen in IBM's US patent 6317114 [18]. Engineers of IBM designed a set of electronic circuits to sense and process displacement signals and then output a signal for the display circuit to adjust the positioning of cathode ray tubes (CRT). In 2009, Rahmati et al. [19] implemented a physics-inspired model, i.e., the mass-spring-damper model, to simulate the IBM circuits in software, and thus enabled display stabilization in modern mobile devices. Here we propose a system modeling-based stabilization technique in this work. With motion prediction, our method can compensate for the handheld shake more precisely. We conduct both accuracy analysis and user tests to verify the feasibility of this stabilization technique.

3. Compensation Based Anti-Shake Mechanism. As Figure 1 shows, the anti-shake mechanism we implement consists of three pipelined units, i.e., the analysis unit, the prediction unit, and the compensation unit. The compensation-based anti-shake mechanism

creates an active area for mobile display. Stabilization, thus, results from moving the active area on the screen.

3.1. Workflow of the anti-shake process. We provide four operation-based arguments to enhance this mechanism, i.e., the border space “ b ”, the scale factor “ c ”, the suspending time “ t ”, and the moving bound “ d ”. Argument b indicates the moving range from the edge of the screen to the active display area. If b is assigned a value of zero, the active zone will move without buffers. Argument c is a scale factor that allows users to adjust the scale for each compensation move. Argument t introduces a period where the compensation process is not run. The timer of this period will reset and the active area will return to the center of the screen whenever the screen is touched or when the device is shaken with a displacement that is greater than the defined threshold, d . In this way, the user can interact with the mobile device in a normal manner.

The entire cycle for stable display is as follows. First, the analysis unit reads the accelerometer. The acceleration is divided into X and Y components and adjusted, following measurements made with the gyroscope, to remove the effects of gravity. In the current version of implementation, we read the type of *linear acceleration* that excludes the gravity directly. The prediction unit then processes X and Y data separately and estimates the next displacement of the mobile device along these two axes. Finally, the compensation unit moves the active display area in the opposite directions. The operation arguments b , c , t , and d function in the compensation unit, i.e., compensative moving therein has to take care of the border space, the scale factor, the suspending time, and the moving bound. For the prediction unit, the technical details are described below.

3.2. System modeling-based prediction. Before we can use the system modeling method to predict the movement of the mobile device, we have to calculate the displacement signal as a function of the acceleration signal. We process X and Y data separately; the estimation equation that applies to both X and Y axes is given by Equation (1), where a and D sequences represent acceleration and the displacement, respectively.

$$D[k] \approx \Delta t \cdot v[k] = \Delta t \cdot (v[k-1] + \Delta t \cdot a[k]) = D[k-1] + (\Delta t)^2 \cdot a[k]. \quad (1)$$

We applied an auto-regressive (AR) model for system modeling and use the weighted recurrent least-squares estimation (LSE) algorithm [20] to calculate the coefficients of the model. The coefficients update in real time and we can, therefore, predict the displacement at each moment. The AR model is established by Equation (2), where the system parameter n indicates the window size of filtering.

$$\hat{D}[k+1] = \sum_{i=0}^{n-1} (\theta_k)_i \cdot D[k-i]. \quad (2)$$

During motion prediction, the coefficients of the AR model is recurrently calculated by the following weighted LSE equations (Equations (3)-(5)), with weight $0 < \lambda \leq 1$.

$$\phi_k = [D[k-1] \ D[k-2] \ \cdots \ D[k-n]]^T, \quad (3)$$

$$P_k = \frac{1}{\lambda} \left(P_{k-1} - \frac{P_{k-1} \phi_k \phi_k^T P_{k-1}}{\lambda + \phi_k^T P_{k-1} \phi_k} \right), \quad (4)$$

$$\theta_k = \theta_{k-1} + P_k \phi_k (D[k] - \phi_k^T \theta_{k-1}). \quad (5)$$

3.3. Motion compensation. The compensation unit takes charge of moving the active display area. As stated above, this unit works following four operation-based arguments,

i.e., the border space b , the scale factor c , the suspending time t , and the moving bound d . The compensatory offset $C[k + 1]$ can be calculated by Equation (6).

$$C[k + 1] = -c \cdot \hat{D}[k + 1]. \tag{6}$$

Practically, we have to convert the offset $C[k + 1]$ from meters to pixels. Figure 2(a) is an example, where we must set the radius as $p = 570$ pixels for a Nexus 9 tablet computer if we attempt to draw a circle with radius $r = 0.05$ meters. Accordingly, if we want to realize the anti-shake mechanism on this device, we have to multiply the compensatory offset by $p/r = 1.14 \times 10^4$ for presenting it in pixels.

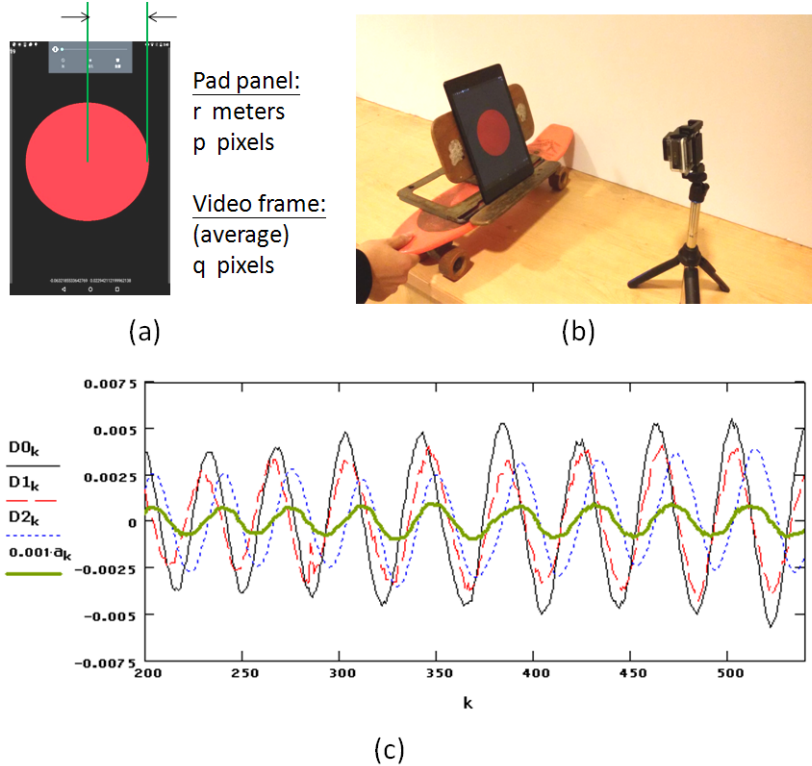


FIGURE 2. Prediction accuracy test: (a) Nexus 9 with a red circle drawn in the center, (b) video captured by a Gopro high frame rate camera, (c) accuracy analysis, where $D0$, $D1$ and $D2$ present the sequences of ground-truth displacements, and the simulated displacements made by our method and [19]’s method, respectively

4. Accuracy Analysis. The kernel of our anti-shake mechanism is the motion prediction technique; therefore, we conducted an experiment to verify the prediction accuracy. Figure 2 shows the process of our experiment. First, we drew a red circle with radius $r = 0.05$ meters on a Nexus 9 tablet computer (Figure 2(a)). We then put this device on a skateboard and placed the skateboard in front of a Gopro high frame rate camera (Figure 2(b)). As we slid the skateboard, the pad device displayed the time above the red circle every second and recorded the acceleration data at 48 Hz. The Gopro camera also captured the video at 48 Hz.

We examined the video frame by frame, and used Hough circle algorithm to detect the centers and the radii of the circles. The move between circle centers on two consecutive frames is the displacement. The average radius of the circle is $q = 172.83$ pixels on the video frames. We can thus convert the ground-truth displacement from pixels to meters

by multiplying $r/q = 2.89 \times 10^{-4}$. The ground-truth displacement sequence D_0 and the acceleration sequence a along X direction can be aligned by the time stamps displayed on the pad panel. These two sequences are drawn in black and bold-brown lines, respectively, in Figure 2(c). We also use our method (with $\lambda = 0.98$ and $n = 12$) and Rahmati's method to generate the displacement sequences, D_1 and D_2 , respectively, on basis of reading the acceleration data. Figure 2(c) shows D_1 and D_2 in dashed-red and dotted-blue lines, respectively.

As we can see on Figure 2(c), our system-modeling-based mechanism outperformed the mass-spring-damper mechanism in simulating the next move. Statistically, the MSEs caused by using these two methods are 1.15×10^{-5} and 2.94×10^{-4} , respectively.

5. Verification by User Tests. Besides the accuracy test, we also developed an Android app for users to test the proposed stabilization technique. Here we implemented the anti-shake mechanism in this app instead of embedding it with the operation system. In this manner, not only can we shorten the response time but also conduct the test on different Android devices. Although the test app displays particular designed contents, it coheres with the workflow we proposed. Thus, one can easily imagine a situation in which an operation system is equipped with the anti-shake mechanism.

The user test verification is as follows. Two runs of three questions were presented to users in the first stage. Each run has (a) a picture-type geometric problem, (b) a text-type math problem, and (c) a video-type counting problem. Figure 3 shows the examples of these questions. After the user takes 12 minutes to answer six questions, he or she

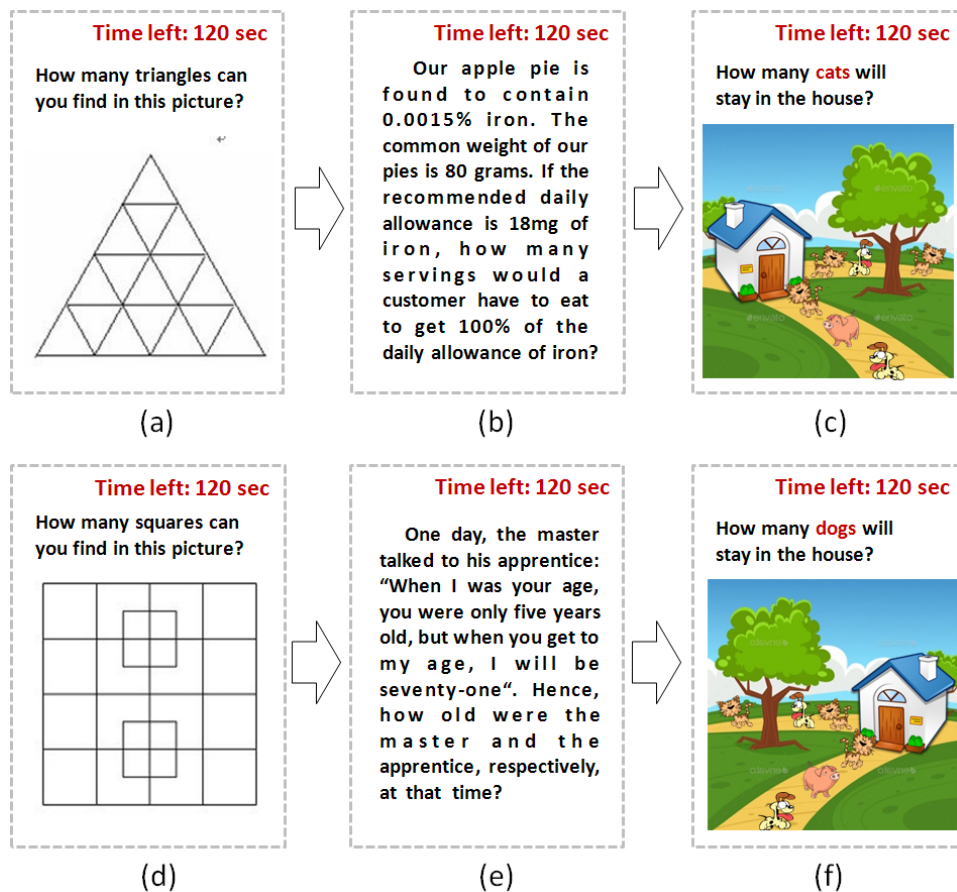


FIGURE 3. Examples of picture type (a and d), text type (b and e), and video type (c and f) questions for users to answer before our tests

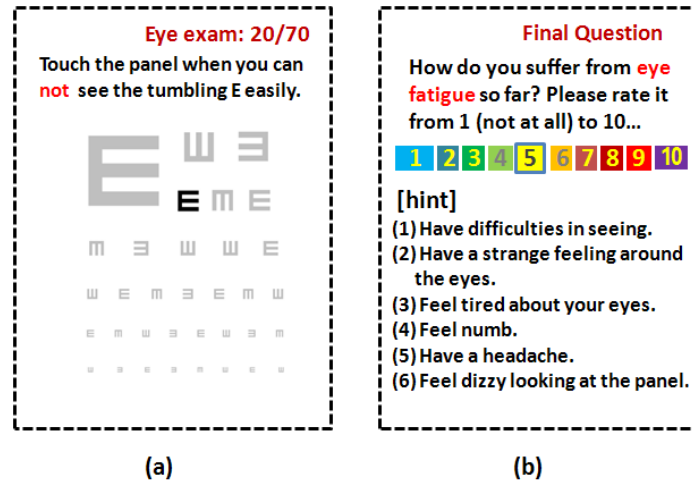


FIGURE 4. User tests – (a) tumbling E eye exam and (b) sight fatigue investigation

is then subjected to a tumbling E eye exam [21] (Figure 4(a)). The distance between the user’s eyes and the screen is maintained at a distance of approximately 40 cm and a 1/15 minified tumbling E chart is presented during this examination. We continuously shrink the focused characters and the user has to touch the screen, at our request, when the characters cannot be seen clearly. Finally, as shown by Figure 4(b), we ask the user whether he or she suffers from visual fatigue as a result of the evaluation. The scores can be given from a range of 1-10, where a higher number represents cases where the user’s vision is compromised [22, 23].

Accuracy in the first six answers is not important for our tests; therefore, only the scores of the tumbling E exams and the 10-point scale questionnaires are recorded. We compare the scores associated with the cases when the anti-shake mechanisms are based on our method, or Rahmati’s method, or turned off. Experimental verification is applied to four different moving environments, i.e., walking, taking a bus, taking the Taipei MRT, and taking the MRT with a side-sitting posture. Again, we selected the hTC Nexus 9 tablet computer as our test device, because it complies with the standard Android 6.0 operation system. The system parameters in Equations (2)-(5) were set to $\lambda = 0.98$ and $n = 12$ for the experiments. As for the operation arguments, we set b , c , t and d to values of 3 (cm), 1, 3 (sec) and 6 (cm), respectively.

The sample users included 80 college students with an equal number of males and females. All of the students have normal eyesight, i.e., above 20/20 vision, without or with the use of optical eyewear or corrective procedures. We asked these participants to hold the device regularly. Once the active display area was reset more than 10 times during the test, we terminated the current test and restarted it after 30 minutes. This was under the assumption that a particular user might not make an effort to decrease the handheld vibration. During our experiments, the participants cooperated with this regulation well. We restarted less than four experiments and the average reset times are less than seven. Table 2 lists the test data and the experimental results averaged from the 80 participants. In comparison to the cases where we turned off or used Rahmati’s model as the anti-shake mechanism, the users observed a sharper image when our mechanism functioned. The record of 10-point questionnaires also reveals that our stabilization techniques provided a more comfortable experience in moving environments.

Table 3 shows parts of the raw data of our experiments. Notice that the values regarding both of eye exams and 10-point scale questionnaires are the lower the better. Here we color

TABLE 2. Experimental results of the eye exams and the sight fatigue questionnaires

Mode\Stabilization	Eye Exams (20/F)			10-Point Scale Questionnaires		
	AR	Ref[19]	off	AR	Ref[19]	off
Walking	24.50	26.00	25.50	2.25	3.20	3.35
Bus	21.25	22.50	23.50	2.25	2.45	2.45
MRT	21.00	21.00	23.25	1.60	1.60	1.75
MRT (side-sitting)	23.50	23.75	24.00	1.85	2.00	2.10
Average	22.56	23.31	24.06	1.99	2.31	2.41

TABLE 3. Parts of the raw data of our experiments. Numbers are underlined and colored in red in case that the anti-shake mechanism was not helpful to the users.

Test	Tumbling E Exam (20/F)								10-Point Questionnaires							
Mode	Walking		Bus		MRT		MRT(side-sit)		Walking		Bus		MRT		MRT(side-sit)	
User	On	off	On	off	On	off	On	off	On	off	On	off	On	off	On	off
1	30	30	20	30	15	15	15	20	3	4	2	2	1	1	1	2
2	30	40	20	20	<u>30</u>	<u>15</u>	<u>20</u>	<u>15</u>	1	2	2	4	<u>2</u>	<u>1</u>	<u>3</u>	<u>2</u>
3	30	30	20	20	15	15	20	20	1	2	2	3	1	3	1	2
4	20	20	20	20	20	30	20	20	3	4	1	2	1	1	1	2
5	20	30	20	30	20	20	30	30	2	3	2	2	1	1	2	2
6	30	30	20	20	20	20	20	20	3	3	2	2	2	2	2	2
7	20	20	30	40	30	30	20	20	2	3	1	3	3	2	2	3
8	<u>30</u>	<u>20</u>	<u>30</u>	<u>20</u>	15	15	<u>30</u>	<u>15</u>	2	2	<u>3</u>	<u>2</u>	1	1	<u>2</u>	<u>1</u>
9	15	30	20	20	15	20	<u>40</u>	<u>20</u>	2	4	2	2	1	2	<u>2</u>	<u>1</u>
10	20	20	20	30	20	20	20	30	2	2	1	2	2	3	2	2
11	20	20	20	20	20	20	20	20	2	4	2	3	2	2	2	2
12	20	20	<u>30</u>	<u>20</u>	<u>30</u>	<u>20</u>	<u>30</u>	<u>15</u>	2	4	<u>3</u>	<u>2</u>	<u>4</u>	<u>2</u>	2	2
13	30	30	20	20	20	20	30	20	2	2	2	2	2	2	3	3
14	20	30	20	40	30	30	20	20	2	3	3	3	2	2	2	3
15	20	20	20	20	20	20	30	30	2	3	1	3	2	2	2	2
16	20	30	20	20	20	30	20	30	3	4	2	3	1	2	2	2
17	15	15	15	30	15	20	30	30	2	4	1	4	1	1	1	2
18	15	20	20	20	15	15	20	30	3	4	2	3	1	1	1	2
19	20	20	<u>30</u>	<u>20</u>	20	20	20	20	3	3	<u>2</u>	<u>1</u>	2	2	1	4
20	30	30	20	20	15	20	20	30	2	4	2	3	1	1	2	2
21	20	20	30	20	30	30	20	30	2	4	2	2	1	2	2	2
22	20	40	15	20	15	30	20	20	1	3	1	3	1	1	1	1
23	20	20	20	20	30	30	20	30	3	4	3	2	1	3	3	2
24	20	40	20	30	20	20	20	30	3	3	2	4	2	2	3	3
25	20	20	20	20	30	30	20	20	3	3	2	3	2	2	2	2
26	<u>30</u>	<u>20</u>	30	30	<u>30</u>	<u>15</u>	<u>20</u>	<u>15</u>	<u>3</u>	<u>2</u>	<u>3</u>	<u>2</u>	<u>2</u>	<u>1</u>	2	2
27	20	20	20	20	30	30	20	30	2	4	2	2	1	1	1	2
28	20	30	20	30	20	20	20	20	2	3	2	2	<u>3</u>	<u>2</u>	2	2
29	20	30	30	30	20	20	20	30	3	3	2	3	2	2	2	2
30	20	20	20	20	20	30	30	20	3	3	2	3	1	2	3	2

the numbers in red in case that the anti-shake mechanism did not work well to improve the usage of mobile devices. We observe two notable facts from these data. First, there exist one seventh to one fifth participants who gain opposite effects from the anti-shake mechanism of mobile display. Perhaps, these users have a unique way to operate mobile devices; or, perhaps, their eye-brain systems can easily track handheld shake and thus they do not need the anti-shake mechanism. Discovery of the unknown reason thereof can be an interesting research topic in the future. Second, we also find that the red numbers appear on both sides (eye exams and eye fatigue questionnaires) near-synchronously. This fact implies that a shaper eye sight leads to a lower degree of eye fatigue.

6. Conclusions. We implemented an anti-shake mechanism to improve the experience of using a mobile device in moving environments. This mechanism relies on three pipelined units, which take charge of motion analysis, motion prediction, and motion compensation, respectively. In this paper, we proposed a system modeling-based technique for motion

prediction. We conducted accuracy analysis and user evaluation to validate the anti-shake mechanism. In the accuracy test, we used a high frame rate camera to capture the process while moving the mobile computer. We then analyzed the ground-truth displacement frame by frame and found that the proposed mechanism can precisely simulate ground-truth displacement sequence after reading acceleration data. In the user evaluation test, users had to look at the screen, at our request, to answer two runs of three picture-type, text-type, and video-type questions. Then we conducted tumbling E exams and 10-point scale questionnaires to these participants. Experimental results reveal that the anti-shake mechanism successfully helped deliver sharp visual content and decreased eye fatigue in moving environments.

The compensation-based anti-shake mechanism, as what we implemented, has its advantages and disadvantages. Firstly, motion compensation is not only valid for displaying text segments but also available for displaying any kind of media. Meanwhile, this method shrinks the display area and thus may lower its acceptance by users. The implementation of this mechanism still has other problems, namely, how to decrease the consumption of power and computing resources, and how to improve the prediction accuracy of the next move. These problems require further research in the future. We may need to develop a hardware optimization to address resource consumption at the circuit level. We may also analyze the moving types and suggest optimal operation-based arguments to users based on the findings. By doing this, we are likely to increase the prediction accuracy.

Acknowledgment. This work was supported in part by the Ministry of Science and Technology, Taiwan (grant no. MOST 105-2221-E-182-082) and Chang Gung Memorial Hospital (grant nos. NERPD2F0381 and BMRPB21). Jyh-Da Wei is also with the Ophthalmology Department, Keellung Chang Gung Memorial Hospital as an assistant research fellow since 2017.

REFERENCES

- [1] P. Pangaro, *The Role of Mobile Computing in Daily Life*, SKP Session – Bell Labs Applications Domain Group, Villarceaux, Nozay, France, 2010.
- [2] R. W. Connolly, Beyond good and evil impacts: Rethinking the social issues components in our computing curricula, *Proc. of the 16th Annual Joint Conference on Innovation and Technology in Computer Science Education*, pp.228-232, 2011.
- [3] R. W. Connolly, Criticizing and modernizing computing curriculum: The case of the web and the social issues courses, *Proc. of the 17th Western Canadian Conference on Computing Education*, pp.52-56, 2012.
- [4] C. Taneja, The psychology of excessive cellular phone use, *Delphi Psychiatry Journal*, vol.17, no.2, pp.448-451, 2014.
- [5] A. J. A. M. van Deursen, C. L. Bolle, S. M. Hegner and P. A. Kommers, Modeling habitual and addictive smartphone behavior: The role of smartphone usage types, emotional intelligence, social stress, self-regulation, age, and gender, *Computers in Human Behavior*, vol.45, pp.411-420, 2015.
- [6] M. Beranuy, U. Oberst, X. Carbonell and A. Chamarro, Problematic Internet and mobile phone use and clinical symptoms in college students: The role of emotional intelligence, *Computers in Human Behavior*, vol.25, pp.1182-1187, 2009.
- [7] T. A. Stoffregen, Y.-C. Chen and F. C. Koslucher, Motion control, motion sickness, and the postural dynamics of mobile devices, *Experimental Brain Research*, vol.232, pp.1389-1397, 2014.
- [8] M. Vinnikov, R. S. Allison and D. Swierad, Real-time simulation of visual defects with gaze-contingent display, *Proc. of the 2008 Symposium on Eye Tracking Research & Applications*, pp.127-130, 2008.
- [9] R. S. Wagner, Smartphones, video display terminals, and dry eye disease in children, *Journal of Pediatric Ophthalmology and Strabismus*, vol.51, p.76, 2014.
- [10] S. Liu, L. Yuan, P. Tan and J. Sun, Bundled camera paths for video stabilization, *ACM Trans. Graphics*, vol.32, pp.78:1-78:10, 2013.

- [11] N. Mansurov, Lens stabilization vs in-camera stabilization, *Photographylife: Articles, News, Reviews*, 2012.
- [12] R. Fergus, B. Singh, A. Hertzmann, S. T. Roweis and W. T. Freeman, Removing camera shake from a single photograph, *ACM Trans. Graphics*, vol.25, pp.787-794, 2006.
- [13] C. Tang, X. Yang, L. Chen and G. Zhai, A fast video stabilization algorithm based on block matching and edge completion, *Proc. of IEEE 13th International Workshop on Multimedia Signal Processing*, pp.1-5, 2011.
- [14] L. Barnard, J. S. Yi, J. A. Jacko and A. Sears, Capturing the effects of context on human performance in mobile computing systems, *Personal and Ubiquitous Computing*, vol.11, pp.81-96, 2007.
- [15] S. K. Kane, J. O. Wobbrock and I. E. Smith, Getting off the treadmill: Evaluating walking user interfaces for mobile devices in public spaces, *Proc. of the 10th International Conference on Human Computer Interaction with Mobile Devices and Services*, pp.109-118, 2008.
- [16] Z. Li, S. Pundlik and G. Luo, Stabilization of magnified videos on a mobile device for visually impaired, *Proc. of Computer Vision and Pattern Recognition Workshops*, pp.54-55, 2013.
- [17] M. Goel, L. Findlater and J. Wobbrock, Walktype: Using accelerometer data to accomodate situational impairments in mobile touch screen text entry, *Proc. of SIGCHI Conference on Human Factors in Computing Systems*, pp.2687-2696, 2012.
- [18] B. Abali, H. Franke and M. Giampapa, Method and apparatus for image stabilization in display device, *US Patent 6,317,114*, 2001.
- [19] A. Rahmati, C. Shepard and L. Zhong, Noshake: Content stabilization for shaking screens of mobile devices, *Proc. of 2009 IEEE International Conference on Pervasive Computing and Communications*, pp.1-6, 2009.
- [20] C. A. Kluever, *Dynamic Systems: Modeling, Simulation, and Control*, 1st Edition, WILEY, 2015.
- [21] P. Kovacs, K. Lackner, A. Barsi and A. Balazs, Measurement of perceived spatial resolution in 3D light-field displays, *Proc. of the 4th IEEE International Conference on International Image Processing*, pp.768-772, 2014.
- [22] H. Heuer, G. Hollendiek, H. Kröger and T. Römer, Die ruhelage der augen und ihr einfluß auf beobachtungsabstand und visuelle ermüdung bei bildschirmarbeit, *Zeitschrift für Experimentelle und Angewandte Psychologie*, vol.36, pp.538-566, 1989.
- [23] H. Rajabi-Vardanjani, E. Habibi, S. Pourabdian, H. Dehghan and M. Maracy, Designing and validation a visual fatigue questionnaire for video display terminals operators, *International Journal of Preventive Medicine*, vol.5, pp.841-848, 2014.